Functional Analysis of a Human Homologue of the *Drosophila* Actin Binding Protein Anillin Suggests a Role in Cytokinesis

Karen Oegema,* Matthew S. Savoian,§ Timothy J. Mitchison,‡ and Christine M. Field‡

*Cell Biology Program, European Molecular Biology Laboratory, Heidelberg, Germany D-69117; ‡Department of Cell Biology, Harvard Medical School, Boston, Massachusetts 02115; §Division of Molecular Medicine, New York State Department of Health, Wadsworth Center, Albany, New York 12201-0509

Abstract. We have characterized a human homologue of anillin, a *Drosophila* actin binding protein. Like *Drosophila* anillin, the human protein localizes to the nucleus during interphase, the cortex following nuclear envelope breakdown, and the cleavage furrow during cytokinesis. Anillin also localizes to ectopic cleavage furrows generated between two spindles in fused PtK_1 cells. Microinjection of antianillin antibodies slows cleavage, leading to furrow regression and the generation of multinucleate cells. GFP fusions that contain the COOH-terminal 197 amino acids of anillin, which includes a pleckstrin homology (PH) domain, form ectopic cortical foci during interphase. The septin Hcdc10 localizes to these ectopic foci, whereas myosin II and actin do not, suggesting that anillin interacts with the septins at the cortex. Robust cleavage furrow localization requires both this COOH-terminal domain and additional NH_2-terminal sequences corresponding to an actin binding domain defined by in vitro cosedimentation assays. Endogenous anillin and Hcdc10 colocalize to punctate foci associated with actin cables throughout mitosis and the accumulation of both proteins at the cell equator requires filamentous actin. These results indicate that anillin is a conserved cleavage furrow component important for cytokinesis. Interactions with at least two other furrow proteins, actin and the septins, likely contribute to anillin function.

Key words: Hedc10 • pleckstrin homology domain • septin • cleavage furrow • cortex

Introduction

Cytokinesis is the process that partitions the cell surface and cytoplasm of one cell to form two cells (for reviews see Glotzer, 1997; Gould and Simanis, 1997; Field et al., 1999; Hales et al., 1999). To avoid aneuploidy, the cell must successfully coordinate cytokinesis with chromosome segregation. In animal cells, this coordination is achieved, in part, by assembling the cleavage furrow in response to signals from the late anaphase spindle. The exact nature of this signaling remains poorly understood.

In animal cells, the cytoplasm is partitioned by ingression of the cleavage furrow. Cleavage furrow ingression requires a contractile cortical ring of actin and myosin II (for review see Satterwhite and Pollard, 1992; for some more recent examples of the role of myosin II during cytokinesis see Bi et al., 1998, and Lippincott and Li, 1998 [*Saccharomyces cerevisiae*]; Shelton et al., 1999 [*Caenorhabditis elegans*]; and Benzanilla et al., 2000 [*Schizosaccharomyces pombe*]). Based on EM studies, filamentous actin and myosin II within the cleavage furrow have been proposed to have a purse string-like organization (for review see Satterwhite and Pollard, 1992). However, more recent work in tissue culture cells and *Dictyostelium* have called this organization into question (Fukui and Inoue, 1991; Fishkind and Wang, 1993; Fishkind et al., 1996; for review see Fishkind and Wang, 1995). Further work is necessary to clarify the organization of actin and myosin II in different systems, and to relate this organization to the contractile forces generated during cytokinesis. The mechanisms that lead to furrow assembly and that allow the contractile ring to remain associated with the plasma membrane during contraction are also topics of current investigation.

In addition to cortical contraction, cleavage furrow ingression requires new membrane insertion. A role for syntaxin-mediated membrane fusion has been demonstrated during cytokinesis in *Arabidobsis* (Lauber et al., 1997) and *C. elegans* (Jantsch-Plunger and Glotzer, 1999), and, during cellularization, a cytokinesis-related furrowing process in *Drosophila* embryos (Burgess et al., 1997). Nevertheless, for furrowing events in most animal sys-

Address correspondence to Karen Oegema, Cell Biology Program, European Molecular Biology Laboratory, Meyerhofstrasse 1, Heidelberg, Germany D-69117. Tel.: 49-6221-387-337. Fax: 49-6221-387-512. E-mail: karen.oegema@embl-heidelberg.de

tems, it is not known exactly where and when this membrane insertion occurs and to what extent membrane insertion is coupled temporally and spatially to furrow ingression. In principle, insertion of a new plasma membrane could occur anywhere on the surface of the cell. Membrane insertion could also occur before contraction and be stored in structures such as microvilli until additional surface area is required (Fullilove and Jacobson, 1971; Turner and Mahowald, 1977). The process of membrane insertion during cleavage has been studied most extensively in *Xenopus* embryos (Bluemink and de Laat, 1973; Danilchik et al., 1998). Here, membrane insertion is coupled to furrow ingression and occurs immediately behind the furrow tip. Membrane insertion in this system requires a specialized MT array, disruption of which can lead to contraction in the absence of membrane insertion, causing the embryo to rupture (Danilchik et al., 1998). However, the *Xenopus* embryo is an extremely large and specialized cell, so it is not clear to what extent mechanisms of membrane deposition will be similar in other systems such as vertebrate somatic cells.

One approach to understanding furrow assembly and ingression is to identify the protein components of the cleavage furrow and the interactions between them, and then study the regulation of these interactions in space and time. A number of cleavage furrow components have now been discovered, and some are evolutionarily conserved. Conserved cleavage furrow components include the following: actin, myosin II, formin homology proteins and IQGAP family members (thought to regulate actin dynamics), and the septin family of small GTPases (for review see Field et al., 1999). The septins are found in large protein complexes containing multiple septin family members that can polymerize to form filaments in vitro (for review see Field and Kellogg, 1999).

Another cleavage furrow component that is likely to function during cytokinesis is anillin. Anillin is a *Drosophila* actin binding protein identified by actin affinity chromatography of embryo extracts. Unlike the septins, actin, and myosin II, anillin specifically localizes to the contractile ring during cytokinesis, and is not found in other contractile actin-rich assemblies such as the stress fibers of cultured cells (Cramer et al., 1997; Kinoshita et al., 1997) or the apical portions of constricting epithelial cells (Young et al., 1991; Fares et al., 1995). This specificity suggests a special role in cell division and has made it a useful cytological marker for cleavage furrows in *Drosophila* (Field and Alberts, 1995; Hime et al., 1996; Adams et al., 1998; Giansanti et al., 1999). Although the molecular function of anillin is not clear, the fact that *Drosophila* anillin binds to, and bundles, actin filaments in vitro, suggests it might be a structural component of the cleavage furrow. The movement of anillin from the interphase nucleus to the cleavage furrow would also be consistent, however, with a role in the largely unknown pathways that signal where and when the furrow assembles. For this reason, we have conducted a phylogenetic and functional analysis of anillin—asking which domains are conserved in evolution, with which other furrow components it interacts, and how these interactions are regulated—with the hope that this information will shed light on the mechanism of cytokinesis.

Materials and Methods

Buffers

CBS: 10 mM MES, 138 mM KCl, 3 mM $MgCl_2$, 2 mM EGTA, and 320 mM sucrose. TBS: 0.15 M NaCl, and 20 mM Tris-Cl, pH 7.4. TBST: TBS + 0.1% Triton X-100. AbDil: TBST, 2% BSA, and 0.1% sodium azide. Mounting media: 0.5% p-phenylenediamine, 20 mM Tris-Cl, pH 8.8, and 90 or 70% glycerol as indicated. Sample buffer: 62.5 mM Tris-Cl, pH 6.8, 3% SDS wt/vol, 5% β-ME vol/vol, and 10% glycerol vol/vol. Transfer buffer: 20 mM Tris base, 216 mM glycine, and 20% methanol.

Cloning and Sequencing of a Human Anillin cDNA

A BLAST search of the GenBank database of expressed sequence tags (dbEST) revealed a human cDNA (accession No. R12261) with homology to the COOH terminus of *Drosophila* anillin. PCR primers based on this sequence (ACGCAAGAATCCCATAGG and GACAGCCAGTTCTTGGTAAAC) were used to amplify a 193-bp region, using human HeLa cell QUICK-Clone cDNA (CLONTECH Laboratories, Inc.) as a template. Using this probe, screening of a Uni-Zap XR Library (HeLa cDNA; Stratagene) yielded three related clones, the longest of which (4,016 bp) was sequenced. An additional 559 bp of coding sequence and an upstream, in-frame stop codon were identified using a 5′/3′ RACE kit (Boehringer) and mRNA isolated from HeLa cells using a Quickprep mRNA purification kit (Amersham Pharmacia Biotech) to amplify the 5′ end of human anillin.

GFP Constructs

To generate a fusion of green fluorescent protein (GFP)[1] with amino acids 231–1,125 of human anillin (hsanillin), the KpnI-ApaI fragment from the hsanillin cDNA was ligated into pEGFP-C1 (CLONTECH Laboratories, Inc.). To make (GFP: 231-982, this construct was digested with EcoRI, and the resulting fragment was ligated into pEGFP-C1 cut with EcoRI. To make the full-length construct, GFP: 1-1125, nested PCR using the *Pfu* polymerase (Stratagene) and a human cDNA library (CLONTECH Laboratories, Inc.) as a template was used to amplify the NH_2 terminus of hsanillin. The internal primers were 5′-CGCACGCAAGCTTCGATGGATCCGTTTACGG-3′ and 5′-AGACGCATCATCAGCACTTG-3′. This product was digested with HindIII-BstXI and cloned into the GFP: 231-1125–containing vector. To make GFP: 1-982, the HindIII-BstXI PCR fragment was ligated into GFP: 231-982 cut with the same enzymes. To make all other GFP fusions, PCR with Vent polymerase (New England Biolabs) was used to amplify the appropriate regions. All fragments were digested with HindIII-BamHI and ligated into pEGFP-C1.

Cell Culture and Transfection

BHK-21 cells were cultured and transfected as described (Heald et al., 1993). BS-C-1 (African green monkey kidney) cells were cultured in DME with high glucose. For the blot in Fig. 4, BHK cells were transfected in 6-well plates. The cells were washed twice with PBS and resuspended in 150 μl of sample buffer. 25 μl of each sample was fractionated on a 12% SDS-PAGE gel and Western blotted using an anti-GFP antibody (gift from Aaron Straight, Harvard Medical School, Boston, MA).

Antibody Purification and Labeling

Rabbit antibodies to human anillin were raised against a fusion of GST with amino acids 454–724 of human anillin. To purify the antibodies, the fusion protein was cleaved with Precision protease (Amersham Pharmacia Biotech) to remove the GST and immobilized on Affigel-10 (Bio-Rad Laboratories). The antibodies were purified using standard procedures (Harlow and Lane, 1988). A synthetic peptide corresponding to the COOH-terminal 14 amino acids (SRTLEKNKKKGKIF) of Hcdc10 (Nakatsuru et al., 1994) was used to raise and affinity purify rabbit polyclonal antibodies as previously described (Field et al., 1998). Labeling of antibodies to Hcdc10 and hsanillin with Oregon green (Molecular Probes) and Cy5 (Amersham Pharmacia Biotech) was performed as previously described (Francis-Lang et al., 1999).

[1]*Abbreviations used in this paper:* GFP, green fluorescent protein; hsanillin, human anillin; PH, pleckstrin homology.

Fixation, Immunofluorescence, and Microscopy

For the anillin immunofluorescence in Fig. 1, BHK cells were fixed for 5 min with −20 methanol and processed using standard procedures (http://iccbweb.med.harvard.edu/mitchisonlab/). Antianillin antibodies were used at a concentration of 1 μg/ml. For the visualization of Hcdc10, actin and anillin in Fig. 7, BHK cells, grown on coverslips, were fixed for 15 min in 2% formaldehyde in CBS, washed three times with TBS, permeabilized in TBS + 0.5% Triton X-100 for 10 min, rinsed twice with TBST, and blocked in AbDil for 10 min. The coverslips were incubated with directly labeled Cy-5 antianillin and Oregon green anti-Hcdc10 (both at 2 μg/ml) for 40 min, washed three times with TBST, incubated with 0.05 mg/ml TRITC phalloidin (Sigma Chemical Co.) diluted in AbDil for 15 min, washed twice with TBST, and incubated with 1 μg/ml Hoechst in TBST for 5 min. The coverslips were washed twice in TBST and mounted in mounting media (see Buffers) containing 70% glycerol. BHK cells transfected with GFP constructs (see Figs. 5 and 6) were fixed for 10 min with 2% formaldehyde in CBS. The coverslips were washed, permeabilized, and blocked as described above. To stain for Hcdc10, the cells were incubated with 2 μg/ml of directly labeled Cy5 anti-Hcdc10. Three-dimensional images were acquired on a widefield microscope (DeltaVision; Applied Precision Inc.). Optical sections were taken at 0.2-μm intervals using an Olympus 100×, 1.4 NA objective and deconvolved using the DeltaVision software. Either single optical sections or projections of the entire cell are shown, as indicated.

Antibody Injection Experiments

The day before injection, BS-C-1 cells were plated onto 25-mm coverslips. For injection and viewing, coverslips were mounted in a water-jacketed coverslip chamber to maintain a temperature of 34°C. The chamber was placed on the stage of an inverted microscope and injected and viewed by phase optics. The estimated injection volume is 5% of cell volume. Two different concentrations of affinity-purified antianillin antibody were injected with similar results (3.4 and 11 mg/ml). Random rabbit IgG (Jackson ImmunoResearch Laboratories) at a concentration of 11 mg/ml was injected as a control. For the overnight experiments, interphase cells were injected, and the coverslip was returned to the incubator for 18–22 h. Cells were fixed for 10 min in 2% formaldehyde in PBS and treated as above. Cells were stained with rhodamine-phalloidin (1 μg/ml), Hoechst (2 μg/ml), and fluorescein anti-rabbit IgG. Injected cells were identified by their bright fluorescein staining. For time-lapse filming, single cells were injected at prophase or metaphase and filming began immediately. Images were collected at 20-s intervals. A cell was deemed to have completed cytokinesis when it was no longer possible to make meaningful measurements (i.e., the curvature of the daughters precluded measurement of the intracellular bridge). To determine furrow contraction rates, the distance across the cell at the equator was measured, beginning at anaphase onset. The maximum rate of sustained contraction was determined (times when contraction was stalled were not used in the determination of contraction rate).

Fusion and Microscopy of PTK_1 Cells

Fusion and microscopy of PtK_1 cells was performed as described previously (Savoian et al., 1999). Antianillin antibody was used at a concentration of 4 μg/ml. Cells were fixed ~5 min after formation of the ectopic furrow.

Results

Identification of a Human Homologue of Anillin

Using homology to *Drosophila* anillin, we cloned a human homologue (see Materials and Methods). The human anillin cDNA encodes a 1,125–amino acid protein with a predicted molecular mass of 124 kD and a pI of 8.1. BLAST searches of the databases using the human and *Drosophila* sequences identify four additional proteins with homology to anillin. These include the predicted products of the *Drosophila* gene CG4530 and the *C. elegans* genes, Y49E10.19, K10B2.5, and Y43F8C.14. All six proteins share an extended region of homology at their COOH termini (see alignment in Fig. 1 A). This region includes a COOH-terminal pleckstrin homology (PH) domain (Fig. 1 A, located between 330 and 480 on the ruler) and additional NH_2-terminal sequences (located between 1 and 330 on the ruler) that likely contain an additional conserved globular domain. The NH_2 termini of the six proteins are less conserved. Pairwise alignments (Tatusova and Madden, 1999) indicate that the human and *Drosophila* sequences are homologous along their entire lengths, although the level of conservation is significantly higher in the COOH-terminal third of the protein (Fig. 1 B). The COOH-terminal PH domain is the most conserved part of the protein (54% identity between human and *Drosophila*). Also conserved between the human and *Drosophila* sequences are several consensus nuclear localization sequences (NLSs; Robbins et al., 1991; Hicks and Raikhel, 1995) and one consensus SH3 binding motif (Ren et al., 1993; Lim et al., 1994). In contrast, pairwise alignments reveal no significant homology between the NH_2 termini of the predicted *Drosophila* protein CG4530 or the *C. elegans* protein Y43F8C.14 and the human and *Drosophila* NH_2-terminal sequences. An intermediate level of NH_2-terminal homology is detected between the *C. elegans* proteins, Y49E10.19 and K10B2.5, and the human and *Drosophila* proteins. These results indicate that anillin is conserved among metazoans and that at least some organisms may have more than one protein with homology to anillin. Whether these homologous proteins are functionally redundant or involved in disparate processes remains to be determined.

To further characterize the human anillin homologue, we raised and affinity-purified an antibody to amino acids 454–724 of the human protein. Using this antibody, Western blots of extracts from multiple mammalian cell lines revealed a single band migrating at ~180 kD (Fig. 1 C), which is a molecular mass significantly larger than the predicted molecular mass of 124 kD. A similar difference between the apparent molecular mass and predicted molecular mass was observed for *Drosophila* anillin (see Discussion in Field and Alberts, 1995). The localization of the human protein is essentially the same as that of *Drosophila* anillin (Field and Alberts, 1995). In mammalian tissue culture cells (Fig. 1 D), anillin concentrates in the nucleus during interphase, although some anillin also appears punctate in the cytoplasm and at the cortex. During mitosis, anillin is enriched at the cortex. Anillin accumulates in the cleavage furrow during cytokinesis and prominently stains the cortex surrounding the midbody late in telophase.

The only known molecular interaction of *Drosophila* anillin is to bind to actin filaments in vitro. In the *Drosophila* protein, the actin binding domain has been mapped to the NH_2 terminus (Fig. 1 B). To test if the human protein could also bind actin, fragments of human anillin were expressed and purified from bacteria, and an actin cosedimentation experiment was performed. We found that fragments corresponding to amino acids 1–677 and 231–677 of human anillin bound to actin filaments. More COOH-terminal fragments corresponding to amino acids 454–724 and 983–1,125 of human anillin did not bind actin (data not shown). These results suggest that the minimal actin binding domain for the human protein likely lies between amino acids 231 and 454, similar to its location in the *Dro-*

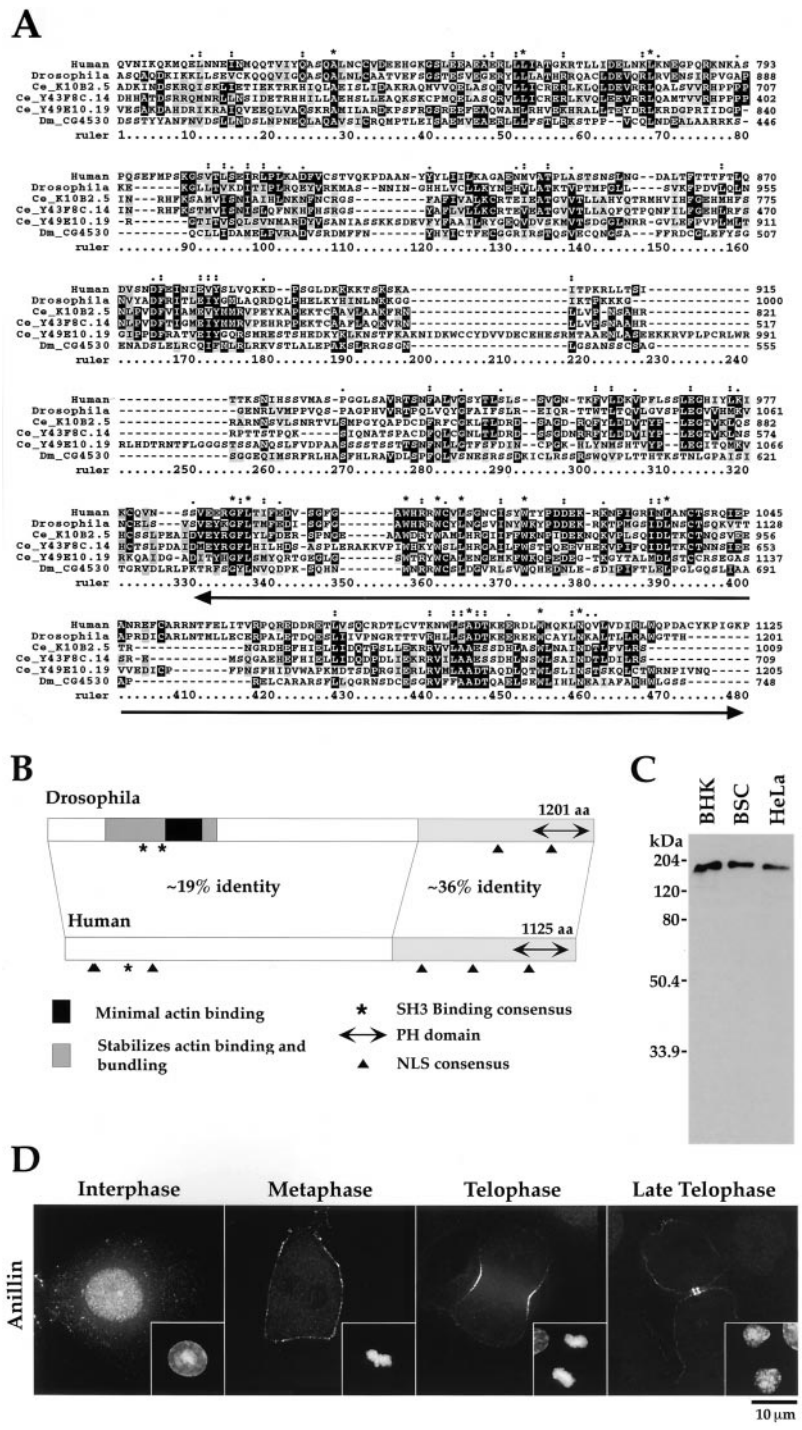

Figure 1. Characterization of an anillin homologue. (A) An alignment of the conserved COOH-terminal region of anillin homologues found in blast searches of the databases. The aligned sequences are human anillin (this report; GenBank accession No. AF273437); *Drosophila* anillin (Field and Alberts, 1995; GenBank accession No. X89858); the products of the *C. elegans* genes K10B2.5 (GenBank accession No. T16604), Y43F8C.14 (GenBank accession No. T26874), and Y49E10.19 (GenBank accession No. T27053); and the product of the *Drosophila* gene CG4530 (GenBank accession No. AAF47044). The sequences were aligned with ClustalX (Thompson et al., 1997) using the default settings. The asterisk indicate positions where the amino acid is identical in all six sequences; a single dot indicates positions where the amino acids of all sequences fall into a weak similarity group; and a double dot indicates positions where the amino acids of all sequences fall into a strong similarity group. The PH domain is underlined. (B) A schematic comparison of *Drosophila* and human anillin homologues. The overall level of identity between the two proteins is 25%. The COOH-terminal third of the protein is the most conserved (~36% identity). This region includes a PH domain (human, amino acids 985–1,110; *Drosophila*, amino acids 1,069–1,194), which is 54% identical between the two proteins. The minimal sequences required for actin binding (amino acids 258–340, indicated here in black) and bundling (amino acids 246–371) have been mapped for the *Drosophila* protein (Field and Alberts, 1995). A larger region of the *Drosophila* protein (amino acids 127–371, shown here in medium gray) was found to stabilize actin binding and bundling. The locations of potential nuclear localization sequences, identified using the program PSORT II (Nakai and Horton, 1999), are indicated with black triangles (human, amino acids 64, 66, 195, 786, 896, and 1,021; *Drosophila*, amino acids 996 and 1,105). Also conserved is a potential SH3 binding motif. There is one SH3 binding consensus in the human and two in the *Drosophila* sequence (indicated here with asterisks). (C) An affinity-purified antibody against hsanillin recognizes a single band in extracts of mammalian cells. A Western blot of cell extracts probed with affinity-purified antibodies to hsanillin. Extracts of BHK-21, BS-C-1, and HeLa cells were loaded. In all cases, a single band running at ~180 kD is detected. (D) hsanillin, like the *Drosophila* protein, has a dynamic cell cycle–dependent localization pattern. Methanol-fixed BHK cells were stained for hsanillin. Three-dimensional widefield data was collected and deconvolved. The interphase cell is a projection of the entire stack; the other images are selected sections. In interphase cells, hsanillin is found primarily in the nucleus, upon nuclear envelope breakdown, hsanillin becomes enriched at the cortex. During cytokinesis, the protein localizes to the cleavage furrow. In late telophase, anillin is concentrated in the cortex surrounding the midbody.

sophila protein. The actin binding of fragment 231–677 was less efficient than that of 1–677, suggesting that, as is the case in *Drosophila*, additional NH_2-terminal sequences may influence actin binding.

Injection of Antibodies to Anillin Slows Furrow Ingression and Leads to Failure of Cytokinesis

To determine if anillin is important for cytokinesis, we injected affinity-purified antibody against human anillin into

monkey cells (BS-C-1). Random rabbit IgG at the same concentration was injected as a control. After injection, the cells were cultured for 18–22 h, fixed, and processed for immunofluorescence (see Materials and Methods). The number of nuclei per cell was counted. 89% (54/61) of the cells injected with the antianillin antibody had two or more nuclei compared with 7% (3/46) of injected control cells. The multinucleate cells resulting from the antianillin injection were well spread and contained actin stress fibers (data not shown). These data suggest a role for anillin in cytokinesis but not cell spreading or cell cycle progression.

A failure of cytokinesis can arise from a failure in furrow assembly, ingression (contraction or perhaps membrane insertion), or from a failure of completion, which is the final step that resolves the contracted cortex to generate two topologically distinct cells. To quantitatively analyze cytokinesis in the antibody-injected cells, cells were injected with antianillin antibody in prophase or metaphase (before formation of the cleavage furrow) and time-lapse–imaged using phase-contrast optics. The width of the furrow near the cell equator was measured and plotted versus time. In all cells injected with anillin antibody, the cleavage furrow formed and began to contract. The timing of furrow initiation was not significantly different between experimental (average 204 ± 31.7 s) and uninjected control cells (average 225 ± 80 s). However, the rate of furrow contraction of the antibody-injected cells was significantly slower ($P < 0.001$; Fig. 2 C) than that of control cells. The rate of furrow contraction of the antibody-injected cells (0.94 ± 0.28 μm/min) was about half that of the control cells (2.09 ± 0.63 μm/min). In 6/9 cells injected with the antianillin antibody, furrow ingression ultimately halted and reversed (Fig. 2). In the three cells where the furrow persisted, ingression eventually stalled and did not reinitiate in the time frame of the experiment (36, 48, and 54 min). Control cells took an average of 9 min to complete cytokinesis. Cumulatively, these results suggest that anillin is important for cytokinesis and may have a role in the assembly, stability, or contractile activity of the cleavage furrow.

Anillin Localizes to Ectopic Rappaport Furrows in Fused PTK_1 Cells

Recently, a system using fused PTK_1 cells was developed to help assess the minimum protein complement necessary to accomplish cytokinesis (Savoian et al., 1999). In fused cells, two spindles exist within one cytoplasm. During cy-

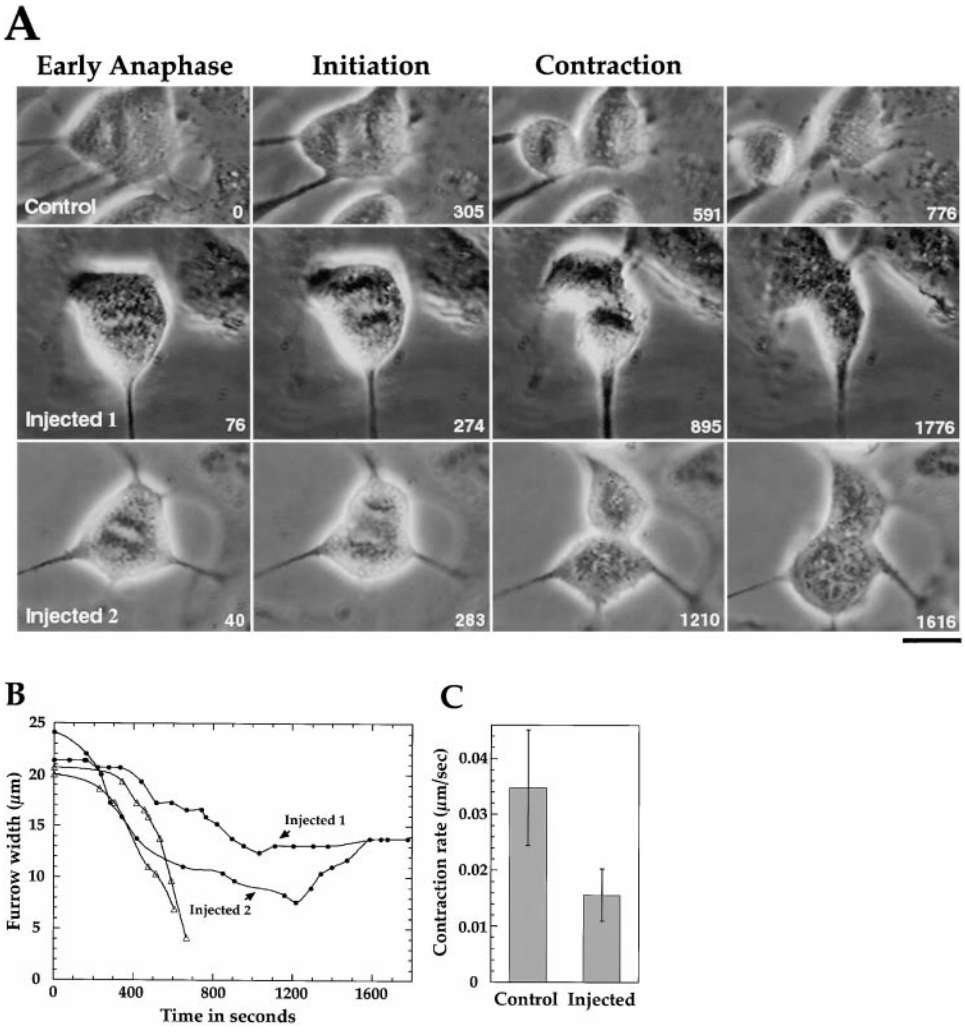

Figure 2. Cytokinesis fails in cells microinjected with antianillin antibody. (A) Selected images from three time-lapse movies. Time (in seconds) from anaphase onset is shown in the bottom right-hand corner of each image. The top row shows an uninjected control cell. In the control, cytokinesis is almost complete in 10 min, and, within 13 min (776 s), the daughter cells have moved apart. The bottom two rows show two examples of cells injected with antianillin antibody. In both cases, furrowing initiates at approximately the same time as in the control cell; however, in each case, ingression stops and cell division fails. (B) Plots of the cell width near the equator with respect to time. Open triangles are control cells and filled circles are antibody-injected cells. The two cells shown in Fig. 2 A are plotted. Injected 1 contracts slowly, stops, and cytokinesis fails. Injected 2 constricts at a faster rate, but the furrow eventually relaxes, opens up, and cell division also fails. (C) Bar graph showing the difference in the maximum rate of contraction between control cells (0.035 ± 0.010 μm/s, $n = 5$) and cells injected with antianillin antibody (0.016 ± 0.0047 μm/s, $n = 8$). Error bars are the SD. Bar, 15 μm.

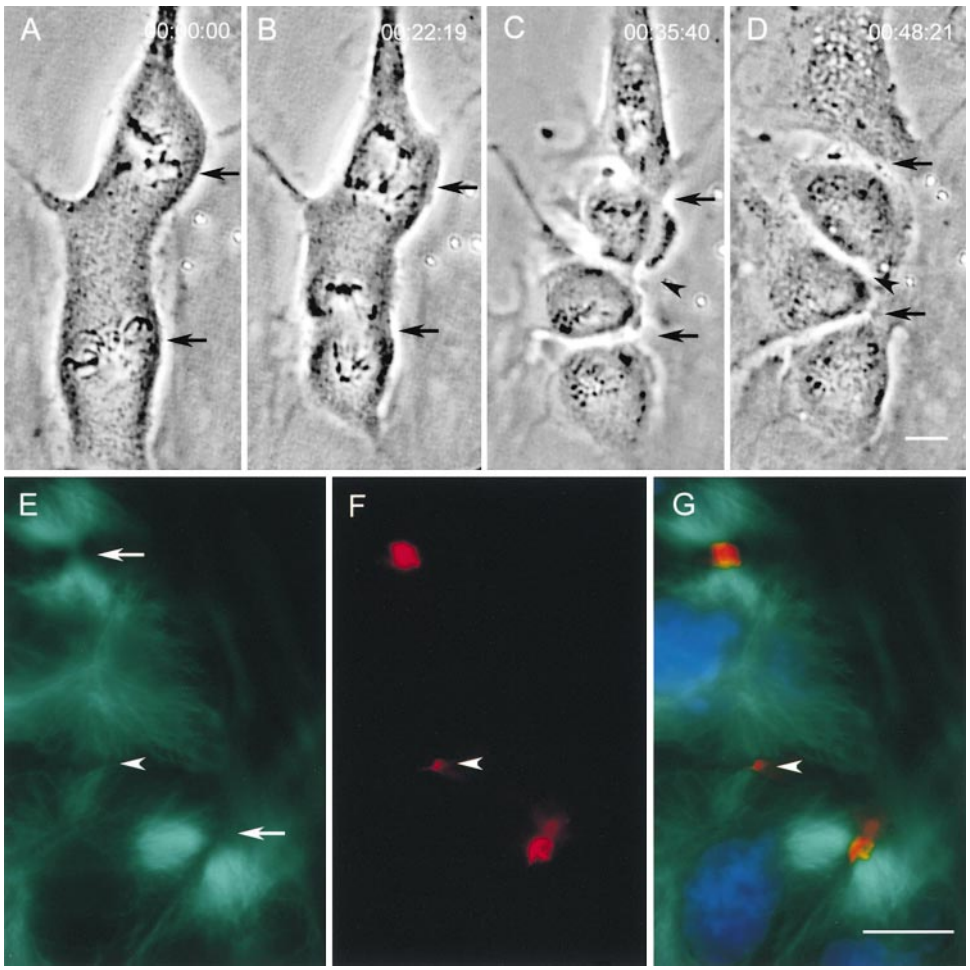

Figure 3. Anillin is found in ectopic furrows that form between asters not previously connected by a spindle in fused PtK_1 cells. (A–D) Selected images from a time-lapse sequence of a PtK_1 heterokaryon, which forms an ectopic midbody between two independent mitotic spindles. Shortly after the onset of cytokinesis at each spindle equator (B, black arrows), an ectopic furrow formed (C, black arrowhead) and progressed to form a midbody (D). (E and F) Indirect immunofluorescence of the same cell fixed ~5 min after image D. (E) Microtubule staining demonstrates that the ectopic midbody contains microtubules (white arrowhead), although fewer than the midbodies, associated with the spindle midzones (white arrows). (F) An analysis of anillin distribution reveals that it is always present at all midbodies including the ectopic (white arrowheads). (G) Merged images of microtubules (green), anillin (red), and DNA (blue). Bars, 10 μm.

tokinesis, three cleavage furrows form: two normal furrows that bisect the spindles, and an ectopic furrow which forms between centrosome pairs not previously connected by a spindle. This type of ectopic furrow was previously characterized in echinoderms by Rappaport (1961). Since both types of furrows are functional, components essential for cleavage should be present in both. In contrast, components that fortuitously accumulate in the cleavage furrow may be found only in spindle-bisecting furrows. We examined the localization of anillin in this system and found that anillin localized to all functional furrows, both spindle bisecting and ectopic, which is consistent with the idea that anillin is a ubiquitous component of cleavage furrows (Fig. 3).

Robust Recruitment of Anillin to the Cleavage Furrow Requires both the PH and Actin Binding Domains

To examine the domains of anillin required for its localization, we transfected BHK cells with a series of constructs that fuse GFP to regions of anillin (summarized in Fig. 4). Fusions of GFP with full-length anillin and anillin lacking the NH_2-terminal 230 amino acids were recruited to the cortex normally during metaphase (Fig. 5, top panel, amino acids 1–1,125 and 231–1,125), and localized robustly to cleavage furrows during cytokinesis (Fig 5, lower panel, amino acids 1–1,125 and 231–1,125). The localization of these two constructs was identical, except that the fusion with amino acids 231–1,125 failed to localize to nuclei during interphase (see summary in Fig. 4). This suggests that the functionally important NLS may be one of the consensus sequences found in the first 230 amino acids (Fig. 1 B). Fusions with amino acids 1–982 or 231–982 that contain the actin binding domain but delete the PH domain were not recruited to the cortex during metaphase (Fig. 5, top panel, amino acids 1–982) and were only very weakly enriched in the cleavage furrow during cytokinesis (Fig. 5, bottom panel amino acids 231–982). Both of these fusions localized to the midbody late in cytokinesis (data not shown). Interestingly, a fusion of GFP with the COOH-terminal 395 amino acids of anillin, which lacks the actin binding domain, showed no cortical enrichment during metaphase (Fig. 5, top panel, amino acids 731–1,125), but was clearly recruited to the cleavage furrow during cytokinesis (Fig. 5, bottom panel, amino acids 731–1,125). Fusions of GFP with smaller regions of the COOH terminus (Fig. 5, bottom panel, amino acids 929–1,125 and 983–1,125) were not recruited to either the cortex during mitosis or the cleavage furrow during cytokinesis. These results suggest that robust recruitment to the cortex and cleavage furrow require both the PH and actin binding domains of anillin. However, a significant amount of cleavage furrow

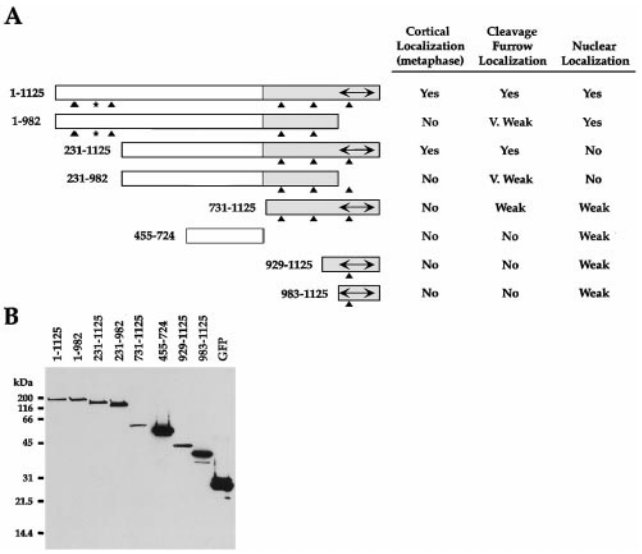

Figure 4. Hsanillin domain analysis. (A) Schematic of the regions of human anillin that were fused to GFP for transfection into BHK cells. All fusions shown here and in the images in Fig. 5 had GFP fused to their NH_2 terminus. However, the full-length protein as well as the regions 455–724, 731–1,125, and 983–1,125 were also tested with GFP fused to their COOH terminus. In all cases, these constructs gave the same localization as the NH_2-terminal fusions. The chart on the right summarizes the localization of the tested fragments. For examples, see Fig. 5. (B) Western blot of cells transfected with each of the NH_2-terminal GFP fusions. Samples were fractionated on a 12% SDS-PAGE gel, transferred to nitrocellulose, and probed with an antibody to GFP.

localization can occur independently of the actin binding domain.

GFP Fusions Containing the Extended PH Domain Form Ectopic Foci that Contain Hcdc10

During interphase, anillin is primarily a nuclear protein. However, we found that all constructs that contained the COOH-terminal 197 amino acids of anillin (Fig. 4, amino acids 929–1,125) could form ectopic cortical foci when overexpressed during interphase (Fig. 6). This region of anillin, which we refer to as the extended PH domain, corresponds to the PH domain plus an additional 56 amino acids more NH_2-terminal. Deletion of the PH domain abolished the ability to form foci, however, the PH domain itself is not sufficient to confer the ability to form these structures (data not shown). We examined the ectopic foci using probes for actin, myosin II, endogenous anillin (us-

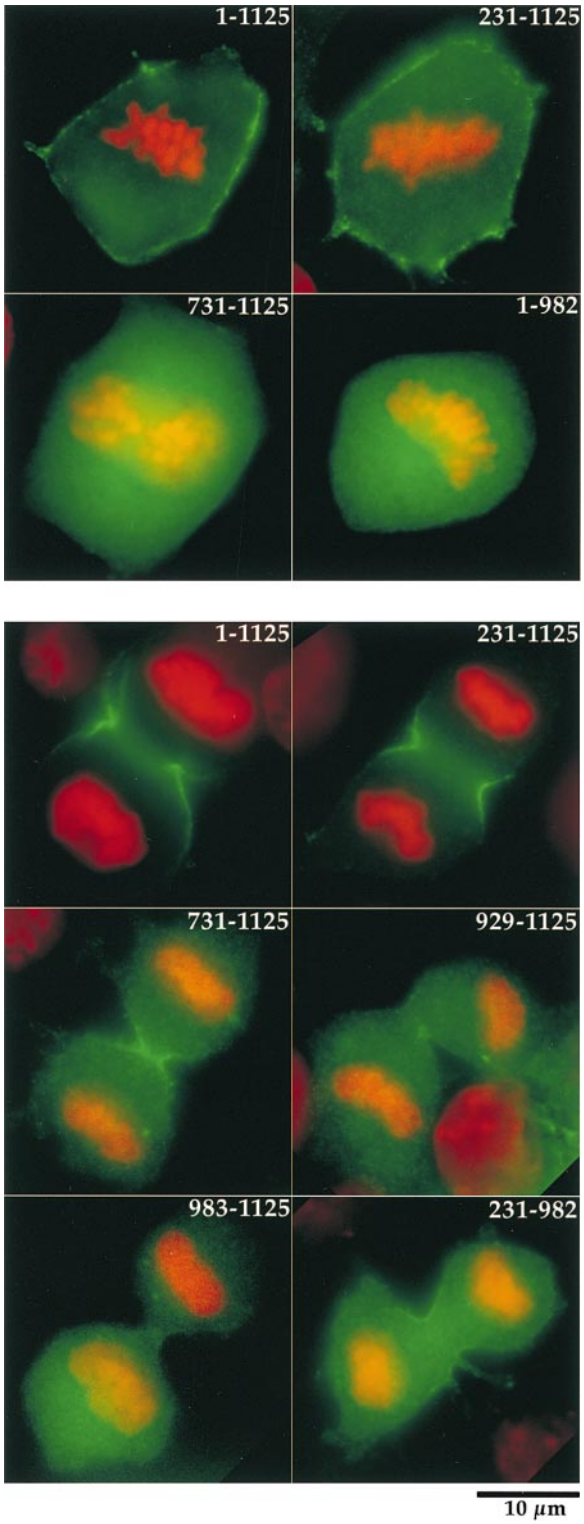

Figure 5. Both the actin binding domain and the PH domain are required for recruitment of anillin to the cortex and for efficient recruitment to the cleavage furrow during cytokinesis. BHK cells were transfected with the indicated GFP constructs and were fixed and stained for DNA. (Top) Cortical recruitment of selected fragments of anillin fused to GFP during metaphase. Full-length anillin (1–1,125) and a fragment, which deletes the first 231 amino acids, are efficiently recruited to the cortex during metaphase. No cortical enrichment of GFP fusions, which delete the actin binding region (731–1,125) or the PH domain (1–982), is observed. (Bottom) Full-length anillin (1–1,125) and a fragment that deletes the NH_2 terminus (231–1,125) are efficiently recruited to the cleavage furrow during cytokinesis. The COOH terminus (731–1,125) is also recruited to the cleavage furrow, but less efficiently. The PH domain alone (983–1,125) or a slightly longer region that contains the PH domain (the extended PH domain, 929–1,125) are not sufficient to direct GFP to the cleavage furrow. GFP fusions that delete only the PH domain (1–982; not shown) or the PH domain and the first 230 amino acids (231–982) were very weakly enriched in the cleavage furrow.

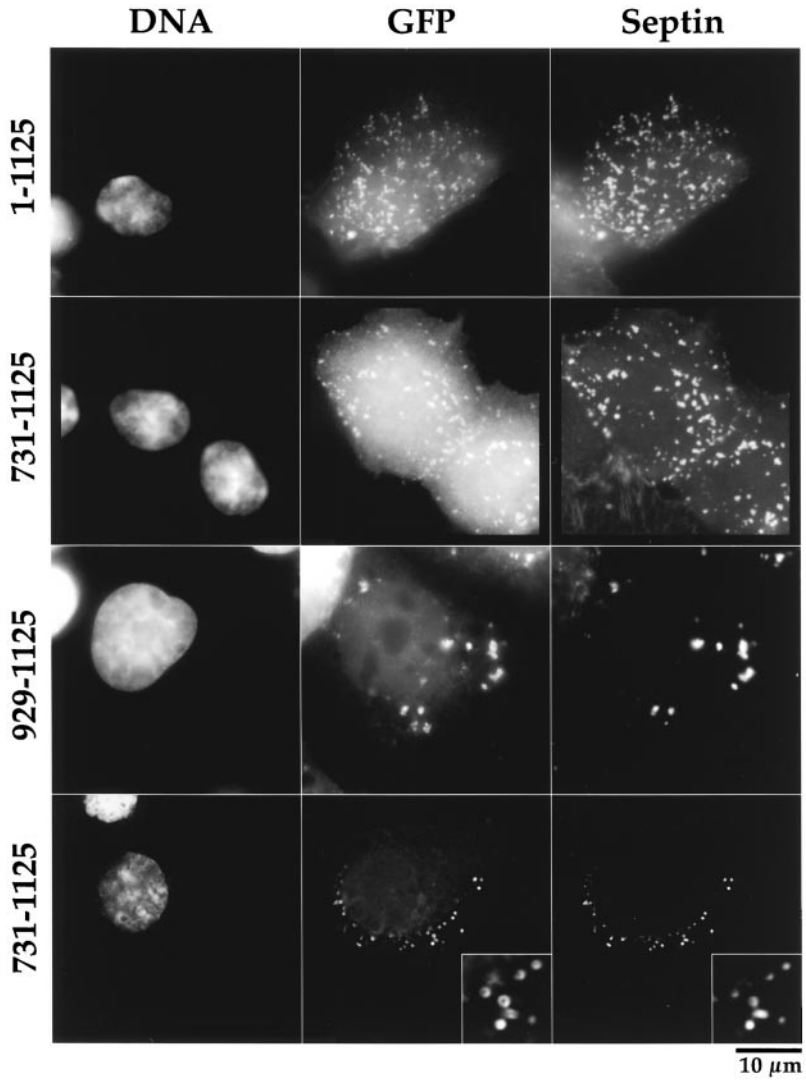

Figure 6. GFP fusions with regions of anillin that contain the COOH-terminal 197 amino acids form ectopic cortical foci during interphase. The septin Hcdc10 also localizes to these foci. BHK cells were transfected with the indicated GFP constructs, fixed, and stained for DNA and the septin Hcdc10. Fusions of GFP with full-length anillin (1–1,125) or with the anillin COOH terminus (731–1,125) form ectopic cortical foci when overexpressed in interphase cells. The septin Hcdc10 localizes to these foci. A fusion of GFP with the COOH-terminal 197 amino acids of anillin (929–1,125) is sufficient to form ectopic foci that colocalize Hcdc10, but these foci tend to be a bit larger and often appear to be beneath the cortex. (Bottom row) Fusions of GFP with the COOH-terminal 395 amino acids of anillin (731–1,125) also often formed ringlike foci. Hcdc10 also colocalized to these rings.

ing an antibody raised against a nonoverlapping fragment), and the septin Hcdc10 (Nakatsuru et al., 1994). This septin is known to localize to cleavage furrows in mammalian cells and to be part of a complex of proteins that has been found to associate with the exocyst complex (Hsu et al., 1998). It is presumably a marker for a complex of septin proteins. Hcdc10 localized to the ectopic foci (Fig. 6), but endogenous anillin, actin, and myosin II did not (data not shown). Hcdc10 localized to the ectopic foci formed by all anillin fusions (Fig. 6). These results suggest that anillin may interact with the septins at the cortex independently of actin or myosin II, and that the extended PH domain (amino acids 929–1,125) is responsible for this interaction. Most constructs formed punctate foci, however, the fusion of GFP with the COOH-terminal 395 amino acids of anillin also formed very homogeneous small rings (Fig. 6, bottom row) with an outer diameter of 0.6 ± 0.04 μm.

Anillin and Hcdc10 Colocalize to Foci Associated with Actin Cables and Are Simultaneously Recruited to the Cleavage Furrow

The GFP fusion data suggested a possible association between anillin and the septins at the cortex. To test if this association could be observed in untransfected cells, we stained BHK cells for actin, Hcdc10, and anillin (Fig. 7) and performed three-dimensional widefield deconvolution microscopy. We found that Hcdc10 and anillin colocalized to punctate cortical structures throughout mitosis. These puncta were smaller than the ectopic cortical foci formed in cells overexpressing GFP-anillin fusions. Nearly all punctate structures that contained anillin also contained Hcdc10. However, some Hcdc10-containing puncta, particularly those outside the cleavage furrow and near the periphery of the cells did not contain anillin (Fig 7; Late anaphase and Telophase). Interestingly, we found that the majority of septin and anillin puncta were aligned along actin cables throughout mitosis. We also observed punctate foci of myosin II aligned along actin cables during furrow assembly (data not shown); but, at our current resolution, myosin II appeared to be less coincident with anillin than Hcdc10. During metaphase and early anaphase, the actin cables appeared to encircle the cells (Fig. 7, Metaphase and Early anaphase). In late anaphase, as the sides of the cells began to flatten to give the cell a capsule-like shape, the cortical actin cables in the cleavage furrow were pri-

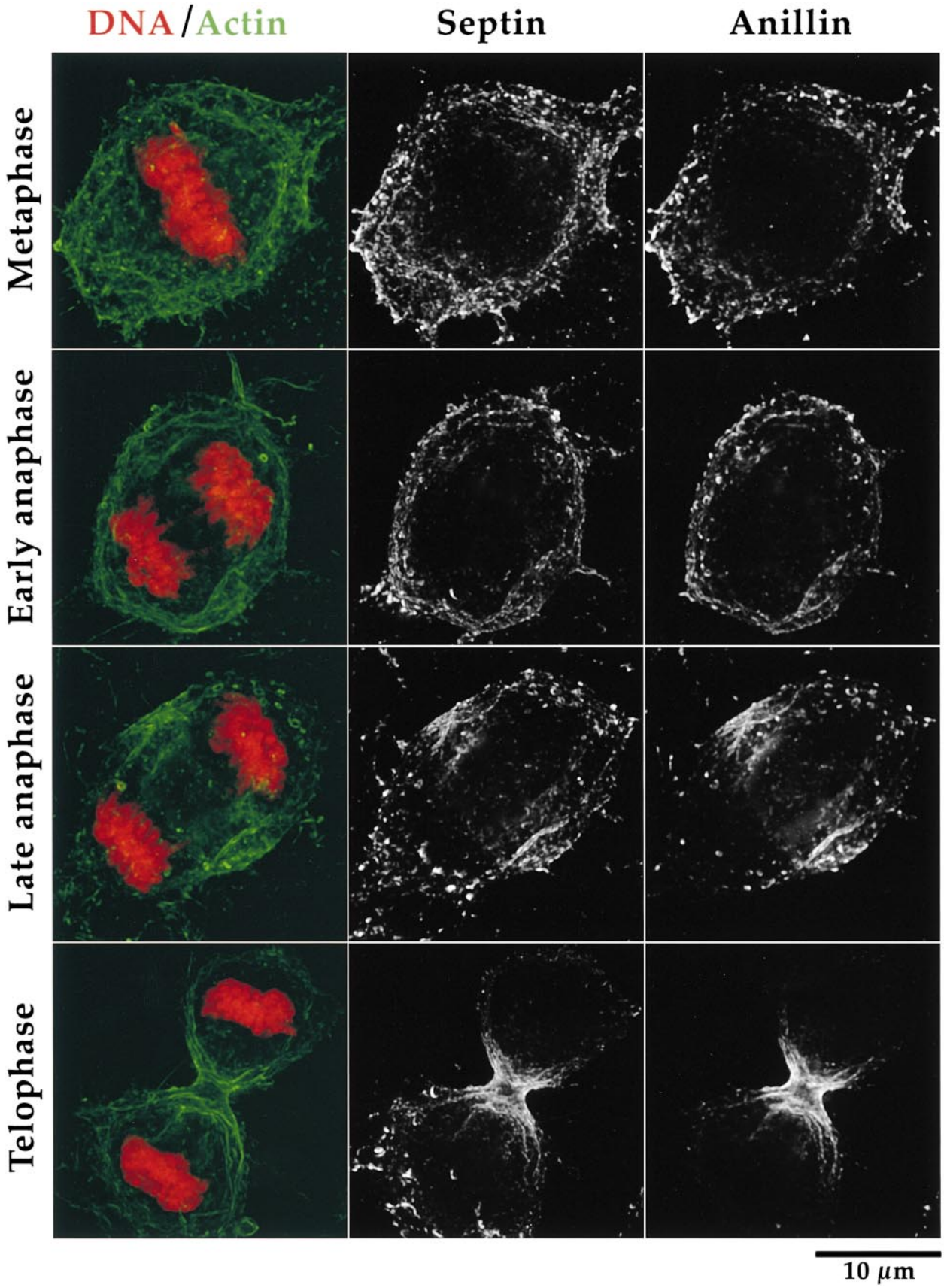

Figure 7. Anillin and Hcdc10 are found in punctate foci that localize along actin cables during mitosis in BHK cells. BHK cells were fixed and stained for actin, Hcdc10, anillin, and DNA. Three-dimensional widefield data sets were collected and deconvolved. Shown are projections of entire cells. During metaphase and early anaphase, actin is found in cables that often appear to encircle the cell. During late anaphase, as the cell initiates contraction, the actin cables appear to align parallel to the spindle axis. As contraction proceeds, more actin cables within the cleavage furrow are observed perpendicular to the spindle axis but, within the actively contracting region near the base of the cell, the actin cables are still parallel to the spindle axis. During all phases of mitosis, anillin and Hcdc10 colocalize to foci that align along actin cables.

marily aligned along the spindle axis. These axially aligned actin filaments appeared to be enriched on the sides of the cell (Fig. 7, Late anaphase), although we also observed them on the top surfaces of some cleavage furrows. Later in telophase, actin cables perpendicular to the spindle axis were also observed. However, these cables were generally enriched to either side of the center of the cleavage furrow and often appeared to encircle the daughter cells rather than to form a circumferential ring at the equator (Fig. 7, Telophase).

We also examined the relative timing of recruitment of anillin and Hcdc10 to the cortex and to the cleavage furrow (a sample field of cells is shown in Fig. 8 A). During interphase, when anillin was primarily nuclear, the septin Hcdc10 was already found in punctate cortical foci. We should note that the nuclear localization of anillin is more prominent in methanol-fixed cells (Fig. 1 D) than in cells fixed with formaldehyde (Fig. 8 A). In metaphase cells, anillin and Hcdc10 colocalize to punctate cortical foci. In anaphase and telophase cells, foci containing anillin and Hcdc10 are found in the cleavage furrow. The timing of cleavage furrow recruitment was identical for the two proteins. Whenever we detected a concentration of one component near the equator, the other was always present. The extent of the region of the cortex where the proteins were enriched was identical throughout furrow assembly and ingression. The timing of furrow recruitment and the extent of the region of enrichment was also identical for myosin II (data not shown).

Anillin and Septins Localize to the Cortex in the Absence of Actin

The localization of anillin and the septin Hcdc10 along actin cables between metaphase and telophase suggested that filamentous actin might be important for their concentration in the furrow. To test if actin filaments are required for anillin and septin localization during cytokinesis, we treated cells with the actin depolymerizing drugs latrunculin A or latrunculin B, fixed, stained, and imaged cells in late mitosis. As expected (Spector et al., 1989), no cleavage furrow was formed in the presence of either drug, and filamentous actin was reduced in amount and disorganized in location (Fig. 8 B). In the absence of a furrow, it is difficult to distinguish anaphase and telophase, but anillin was not localized to the equator in any postanaphase cells we observed after latrunculin A treatment. However, both proteins were still colocalized in foci and largely restricted to the cortex. We conclude that anillin-septin colocalization and maintenance of their association with the cortex do not depend on organized, filamentous actin, whereas their localization to the presumptive cleavage furrow does.

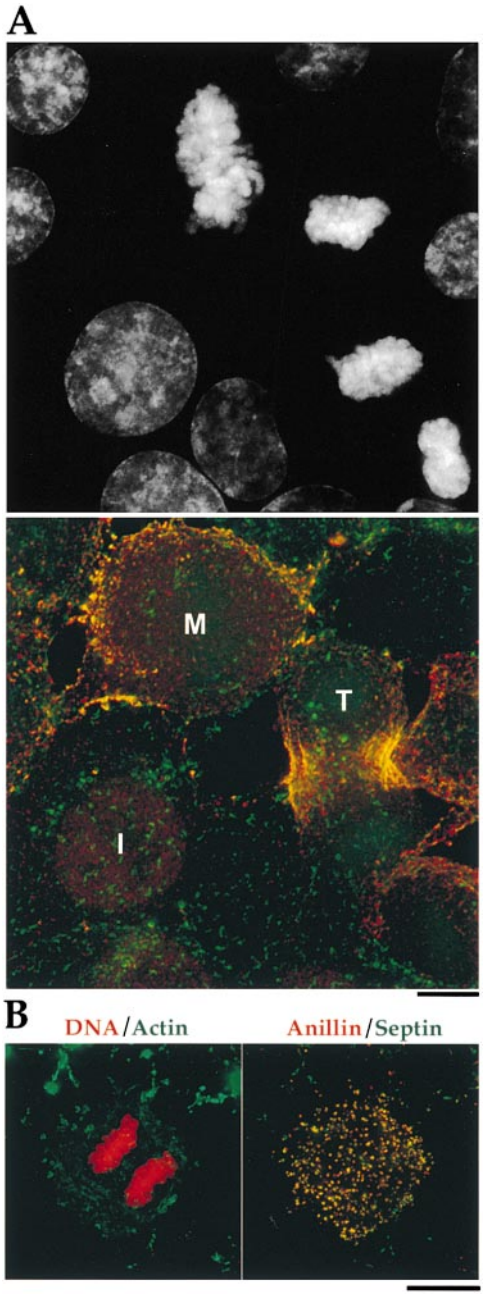

Figure 8. Anillin and the septin Hcdc10 colocalize on the cortex of latrunculin-treated cells but do not accumulate in the cleavage furrow. (A) A typical field of BHK cells fixed and stained for DNA (top), anillin (bottom, red), and Hcdc10 (bottom, green). Three-dimensional widefield data sets were collected and deconvolved. A projection of the field is shown. During interphase (I) Hcdc10 is present in punctate cortical structures on the cortex. Anillin is in the nuclei of most, but not all, interphase cells. Note that the nuclear staining is somewhat weaker in formaldehyde-fixed cells compared with the methanol-fixed cells shown in Fig. 1. At metaphase (M), anillin concentrates at the cortex where it colocalizes with septin foci. At telophase (T), foci containing anillin and Hcdc10 are concentrated in the cleavage furrow. (B) BHK cells grown on coverslips were treated with 2 μg/ml latrunculin A (a gift from Miranda Sanders and Phil Crews, University of California, Santa Cruz) or latrunculin B (Calbiochem) in normal culture media for 60 min before processing for immunofluorescence. In the left panel, a merge of DNA (red) and actin (green) is shown. In the right panels, a merge of anillin (red) and the septin Hcdc10 (green) is shown. Images were collected as described for Fig. 7 and are projections of entire cells. When the actin is depolymerized by latrunculin treatment, neither Hcdc10 nor anillin are recruited to the cell equator during mitosis; instead, they colocalize to large cortical spots.

Discussion

Anillin Is Conserved among Metazoans

Human and *Drosophila* anillin share several conserved features including the presence of consensus nuclear localization and SH3 binding sequences, and a COOH-terminal PH domain. The existence of an anillin homologue in *Xenopus laevis* (Straight, A., personal communication) and of multiple anillin homologues in *C. elegans* (this report) indicates conservation of anillin among metazoans. Although *S. cerevisiae* does not appear to have an anillin homologue, the Mid-1 protein, which is required for septation in the fission yeast *S. pombe*, is similar to anillin in localization (nucleus and cleavage furrow) and also contains a COOH-terminal PH domain. However, there is no other obvious sequence homology (Bähler et al., 1998).

Anillin Function Is Important for Cytokinesis

Injection of antibodies to anillin into mammalian tissue culture cells slows the rate of furrow ingression and prevents the completion of cytokinesis. To more precisely define the pathway in which it acts, it is useful to consider the subprocesses that together comprise cytokinesis (for reviews see Saunders and Field, 1994; Glotzer, 1997; Field et al., 1999). *Initiation*, a signaling process that determines where and when the furrow assembles (for reviews see Rappaport, 1996; Oegema and Mitchison, 1997), is thought to depend on components positioned by the late anaphase spindle microtubules, such as kinesins, kinases, and perhaps chromosomal passenger proteins. Furrow assembly depends on cortical components and the actin cytoskeleton. Furrow ingression can be subdivided into two subprocesses, furrow contraction, which depends on actin and myosin II (for review see Satterwhite and Pollard, 1992) and membrane insertion, which has been shown in a number of systems to require vesicle targeting and exocytic mechanisms (Bluemink and de Laat, 1973; Burgess et al., 1997; Lauber et al., 1997; Danilchik et al., 1998; Jantsch-Plunger and Glotzer, 1999). The relative importance of contraction and membrane insertion during furrow ingression is likely to depend on the system, and has not yet been assessed for vertebrate somatic cells. Finally completion, the process by which the surface area of the cell is finally partitioned, is thought to require midbody microtubules and membrane fusion events (for review see Field et al., 1999). Our localization and antibody injection data suggest that anillin functions during furrow assembly or ingression, and possibly in completion, but not in initiation. Within ingression, we cannot yet determine whether anillin is required primarily for furrow contraction or membrane insertion. The close association of anillin with actin cables in the furrow suggests a role in furrow assembly or contraction. However, the close association of anillin with septins, which have in turn been implicated in exocytotic regulation (Hsu et al., 1998; Beites et al., 1999), suggests that a role in membrane insertion cannot be ruled out.

Functional Domains of Anillin

The Conserved COOH Terminus. Both sequence conservation and localization of GFP fusions suggest a critical role for the COOH-terminal third of anillin (amino acids 731–1,125) that contains the PH domain. When fused to GFP, this domain is sufficient to confer localization to ectopic cortical foci containing the septin Hcdc10 in interphase cells and clear, although relatively weak, localization to the cleavage furrow during cytokinesis. The COOH-terminal PH domain and an additional 56 amino acids NH_2 terminal (amino acids 929–1,125, the extended PH domain) is sufficient to mediate a tight colocalization between anillin and the septins at the cortex during interphase. The full-length endogenous anillin also colocalizes with septins in the cortical foci during mitosis. This colocalization could be explained by a direct physical interaction between the extended PH domain and the septin complex or by cotargeting to some cortical structure without a direct interaction. So far, we have not seen a direct anillin–septin interaction in coimmunoprecipitation experiments. However, these experiments were performed on soluble, as opposed to membrane-bound, protein pools, and the GTP binding status of the septin complex was not manipulated (Oegema, K., and C. Field, unpublished results).

The PH Domain. The COOH-terminal anillin PH domain is necessary for all targeting events, including the formation of ectopic septin–containing foci in cells overexpressing anillin GFP fusions, but is not on its own sufficient to confer any specific localization. PH domains are protein modules of ~120 amino acids thought to mediate recruitment of proteins to the plasma membrane through interactions with lipids (Blomberg et al., 1999). Structural studies indicate that PH domains are electrostatically polarized with a positively charged face that has been postulated to confer the affinity and specificity for different lipids (Lemmon et al., 1996; Rameh et al., 1997). The anillin PH domain is closest in charge to the PH domains of spectrin and dynamin that bind phosphoinositides relatively weakly and nonspecifically. These low affinity PH domains are thought to confer membrane targeting upon oligomerization (Klein et al., 1998) or in conjunction with other domains of the protein (Lemmon et al., 1996). In addition to lipid binding by the anillin PH domain, an interaction with the septins may also be required to target anillin to the cortex. During interphase in BHK cells, the septin Hcdc10 is present on the cortex in the absence of anillin (Fig. 8 A). Anillin may localize to the cortex by targeting to septin-containing cortical structures when released from the nucleus upon entry into mitosis. Cortical targeting of septins may occur by direct association with membranes, as suggested by recent data that the mammalian septin H5 binds specifically to phosphatidylinositol polyphosphate (Zhang et al., 1999).

The NH_2-terminal Actin-binding Domain. Anillin also has a conserved NH_2-terminal actin-binding domain required for both robust cleavage furrow localization and cortical localization at metaphase. Careful colocalization shows that endogenous anillin/septin foci coalign with actin cables throughout mitosis. During cytokinesis, actin cables tend to align along the spindle axis, rather than circumferentially as a simple purse string model might predict. The limitations of the purse string model, and possible implications of noncircumferential actin cables have been discussed elsewhere (Fukui and Inoue, 1991; Fishkind and Wang, 1995). The fact that anillin can bind directly to actin

in vitro makes it an attractive candidate to mediate the alignment of anillin/septin-containing foci along actin cables. However, the possibility that the colocalization of anillin/septin foci along actin cables is mediated by interactions between actin and the septins cannot be ruled out (Kinoshita et al., 1997; Glotzer, 1997). Treatment of cells with actin-depolymerizing drugs abolished the accumulation of anillin and Hcdc10 in the cleavage furrow. However, anillin and the septins remain associated with the cortex in the latrunculin-treated cells, suggesting that maintenance of their cortical localization does not require actin. Experiments examining the kinetics of recruitment will be required to determine if targeting of anillin and Hcdc10 to the cortex can occur normally in the absence of actin.

Cumulatively, our results suggest that anillin may function together with the septins, actin, and myosin II during the assembly and ingression of the cleavage furrow. What might anillin be doing during cytokinesis? Anillin is an actin-binding protein, and fragments of *Drosophila* anillin also bundle actin. Therefore, anillin could have a role in the formation or organization of actin cables in the cleavage furrow or in the dynamics of actin organization during cleavage. Another attractive model is that anillin might mediate interactions between actin and the septin/membrane cytoskeleton, perhaps linking the cleavage furrow to the plasma membrane. These interactions could be important for cleavage furrow assembly or for maintaining structural integrity and membrane attachment of the cleavage furrow during contraction.

Thanks to Arshad Desai (EMBL), John Sisson (University of California, Santa Cruz, Santa Cruz, CA), and Jennifer Tirnauer (Harvard Medical School, Cambridge, MA) for critical reading of the manuscript.

M. Savoian is supported by a National Institutes of Health (NIH) grant GMS R01 40198 (to C.L. Rieder). C. Field is supported by NIH GM 23928 awarded to T. Mitchison. K. Oegema is supported by a postdoctoral fellowship from the Helen Hay Whitney Foundation.

Submitted: 5 April 2000
Revised: 21 June 2000
Accepted: 23 June 2000

References

Adams, R.R., A.A. Tavares, A. Salzberg, H.J. Bellen, and D.M. Glover. 1998. *pavarotti* encodes a kinesin-like protein required to organize the central spindle and contractile ring for cytokinesis. *Genes Dev*. 12:1483–1494.

Bähler, J., A.B. Steever, S. Wheatley, W. Yl, J.R. Pringle, K.L. Gould, and D. McCollum. 1998. Role of polo kinase and Mid1p in determining the site of cell division in fission yeast. *J. Cell Biol*. 143:1603–1616.

Beites, C.L., H. Xie, R. Bowser, and W.S. Trimble. 1999. The septin CDCrel-1 binds syntaxin and inhibits exocytosis. *Nat. Neurosci*. 2:434–439.

Benzanilla, M., J.M. Wilson, and T.D. Pollard. 2000. Fission yeast myosin-II isoforms assemble into contractile rings at distinct times during mitosis. *Curr. Biol*. 10:397–400.

Bi, E., P. Maddox, D.J. Lew, E.D. Salmon, J.N. McMillan, E. Yeh, and J.R. Pringle. 1998. Involvement of an actomyosin contractile ring in *Saccharomyces cerevisiae* cytokinesis. *J. Cell Biol*. 142:1301–1312.

Blomberg, N., E. Baraldi, M. Nilges, and M. Saraste. 1999. The PH superfold: a structural scaffold for multiple functions. *Trends Biochem. Sci*. 24:441–445.

Bluemink, J.G., and S.W. de Laat. 1973. New membrane formation during cytokinesis in normal and cytochalasin B–treated eggs of *Xenopus laevis*. I. Electron microscope observations. *J. Cell Biol*. 59:89–108.

Burgess, R.W., D.L. Deitcher, and T.L. Schwarz. 1997. The synaptic protein syntaxin1 is required for cellularization of *Drosophila* embryos. *J. Cell Biol*. 138:861–875.

Cramer, L.P., M. Siebert, and T.J. Mitchison. 1997. Identification of novel graded polarity actin filament bundles in locomoting heart fibroblasts: implications for the generation of motile force. *J. Cell Biol*. 136:1287–1305.

Danilchik, M.V., W.C. Funk, E.E. Brown, and K. Larkin. 1998. Requirement for microtubules in new membrane formation during cytokinesis of *Xenopus* embryos. *Dev. Biol*. 194:47–60.

Fares, H., M. Peifer, and J.R. Pringle. 1995. Localization and possible functions of *Drosophila* septins. *Mol. Biol. Cell*. 6:1843–1859.

Field, C., R. Li, and K. Oegema. 1999. Cytokinesis in eukaryotes: a mechanistic comparison. *Curr. Opin. Cell Biol*. 11:68–80.

Field, C.M., and B.M. Alberts. 1995. Anillin, a contractile ring protein that cycles from the nucleus to the cell cortex. *J. Cell Biol*. 131:165–178.

Field, C.M., and D. Kellogg. 1999. Septins: cytoskeletal polymers or signalling GTPases? *Trends Cell Biol*. 9:387–394.

Field, C.M., K. Oegema, Y. Zheng, T.J. Mitchison, and C.E. Walczak. 1998. Purification of cytoskeletal proteins using peptide antibodies. *Methods Enzymol*. 298:525–541.

Fishkind, D.J., and Y.L. Wang. 1993. Orientation and three-dimensional organization of actin filaments in dividing cultured cells. *J. Cell Biol*. 123:837–848.

Fishkind, D.J., and Y.L. Wang. 1995. New horizons for cytokinesis. *Curr. Opin. Cell Biol*. 7:23–31.

Fishkind, D.J., J.D. Silverman, and Y.L. Wang. 1996. Function of spindle microtubules in directing cortical movement and actin filament organization in dividing cultured cells. *J. Cell Sci*. 109:2041–2051.

Francis-Lang, H., J. Minden, W. Sullivan, and K. Oegema. 1999. Live confocal analysis with fluorescently labeled proteins. *Methods Mol. Biol*. 122:223–239.

Fukui, Y., and S. Inoue. 1991. Cell division in *Dictyostelium* with special emphasis on actomyosin organization in cytokinesis [published erratum appears in 1991. 19:290]. *Cell Motil. Cytoskelet*. 18:41–54.

Fullilove, S.L., and A.G. Jacobson. 1971. Nuclear elongation and cytokinesis in *Drosophila montana*. *Dev. Biol*. 26:560–577.

Giansanti, M.G., S. Bonaccorsi, and M. Gatti. 1999. The role of anillin in meiotic cytokinesis of *Drosophila* males. *J. Cell Sci*. 112:2323–2334.

Glotzer, M. 1997. The mechanism and control of cytokinesis. *Curr. Opin. Cell Biol*. 9:815–823.

Gould, K.L., and V. Simanis. 1997. The control of septum formation in fission yeast. *Genes Dev*. 11:2939–2951.

Hales, K.G., E. Bi, J.Q. Wu, J.C. Adam, I.C. Yu, and J.R. Pringle. 1999. Cytokinesis: an emerging unified theory for eukaryotes?. *Curr. Opin. Cell Biol*. 11:717–725.

Harlow, E., and D. Lane. 1988. Antibodies: A Laboratory Manual. Cold Spring Harbor Laboratory, Cold Spring Harbor, NY. 726 pp.

Heald, R., M. McLoughlin, and F. McKeon. 1993. Human wee1 maintains mitotic timing by protecting the nucleus from cytoplasmically activated Cdc2 kinase. *Cell*. 74:463–474.

Hicks, G.R., and N.V. Raikhel. 1995. Protein import into the nucleus: an integrated view. *Annu. Rev. Cell Dev. Biol*. 11:155–188.

Hime, G.R., J.A. Brill, and M.T. Fuller. 1996. Assembly of ring canals in the male germ line from structural components of the contractile ring. *J. Cell Sci*. 109:2779–2788.

Hsu, S.C., C.D. Hazuka, R. Roth, D.L. Foletti, J. Heuser, and R.H. Scheller. 1998. Subunit composition, protein interactions, and structures of the mammalian brain sec6/8 complex and septin filaments. *Neuron*. 20:1111–1122.

Jantsch-Plunger, V., and M. Glotzer. 1999. Depletion of syntaxins in the early *Caenorhabditis elegans* embryo reveals a role for membrane fusion events in cytokinesis. *Curr. Biol*. 9:738–745.

Kinoshita, M., S. Kumar, A. Mizoguchi, C. Ide, A. Kinoshita, T. Haraguchi, Y. Hiraoka, and M. Noda. 1997. Nedd5, a mammalian septin, is a novel cytoskeletal component interacting with actin-based structures. *Genes Dev*. 11: 1535–1547.

Klein, D.E., A. Lee, D.W. Frank, M.S. Marks, and M.A. Lemmon. 1998. The pleckstrin homology domains of dynamin isoforms require oligomerization for high affinity phosphoinositide binding. *J. Biol. Chem*. 273:27725–27733.

Lauber, M.H., I. Waizenegger, T. Steinmann, H. Schwarz, U. Mayer, I. Hwang, W. Lukowitz, and G. Jurgens. 1997. The *Arabidopsis* KNOLLE protein is a cytokinesis-specific syntaxin. *J. Cell Biol*. 139:1485–1493.

Lemmon, M.A., K.M. Ferguson, and J. Schlessinger. 1996. PH domains: diverse sequences with a common fold recruit signaling molecules to the cell surface. *Cell*. 85:621–624.

Lim, W.A., F.M. Richards, and R.O. Fox. 1994. Structural determinants of peptide-binding orientation and of sequence specificity in SH3 domains [published erratum appears in 1995. 374:94]. *Nature*. 372:375–379.

Lippincott, J., and R. Li. 1998. Sequential assembly of myosin II, an IQGAP-like protein, and filamentous actin to a ring structure involved in budding yeast cytokinesis. *J. Cell Biol*. 140:355–366.

Nakai, K., and P. Horton. 1999. PSORT: a program for detecting the sorting signals of proteins and predicting their subcellular localization. *Trends Biochem. Sci*. 24:34–35.

Nakatsuru, S., K. Sudo, and Y. Nakamura. 1994. Molecular cloning of a novel human cDNA homologous to CDC10 in *Saccharomyces cerevisiae*. *Biochem. Biophys. Res. Commun*. 202:82–87.

Oegema, K., and T.J. Mitchison. 1997. Rappaport rules: cleavage furrow induction in animal cells. *Proc. Natl. Acad. Sci. USA*. 94:4817–4820.

Rameh, L.E., A. Arvidsson, K.L. Carraway III, A.D. Couvillon, G. Rathbun, A. Crompton, B. VanRenterghem, M.P. Czech, K.S. Ravichandran, S.J. Burakoff, et al. 1997. A comparative analysis of the phosphoinositide binding specificity of pleckstrin homology domains. *J. Biol. Chem*. 272:22059–22066.

Rappaport, R. 1961. Experiments concerning the cleavage stimulus in sand dollar eggs. *J. Exp. Zool*. 148:81–89.

Rappaport, R. 1996. Cytokinesis in Animal Cells. Cambridge University Press,

Cambridge, U.K. 386 pp.
Ren, R., B.J. Mayer, P. Cicchetti, and D. Baltimore. 1993. Identification of a ten-amino acid proline-rich SH3 binding site. *Science.* 259:1157–1161.
Robbins, J., S.M. Dilworth, R.A. Laskey, and C. Dingwall. 1991. Two interdependent basic domains in nucleoplasmin nuclear targeting sequence: identification of a class of bipartite nuclear targeting sequence. *Cell*. 64:615–623.
Satterwhite, L.L., and T.D. Pollard. 1992. Cytokinesis. *Curr. Opin. Cell. Biol.* 4:43–52.
Saunders, S.L., and C.M. Field. 1994. Cell division: septins in common? *Curr. Biol.* 4:907–910.
Savoian, M.S., W.C. Earnshaw, A. Khodjakov, and C.L. Rieder. 1999. Cleavage furrows formed between centrosomes lacking an intervening spindle and chromosomes contain microtubule bundles, INCENP, and CHO1 but not CENP-E. *Mol. Biol. Cell*. 10:297–311.
Shelton, C.A., J.C. Carter, G.C. Ellis, and B. Bowerman. 1999. The nonmuscle myosin regulatory light chain gene mlc-4 is required for cytokinesis, anterior-posterior polarity, and body morphology during *Caenorhabditis elegans* embryogenesis. *J. Cell Biol.* 146:439–451.
Spector, I., N.R. Shochet, D. Blasberger, and Y. Kashman. 1989. Latrunculins—novel marine macrolides that disrupt microfilament organization and affect cell growth: I. Comparison with cytochalasin D. *Cell Motil. Cytoskelet.* 13:127–144.
Tatusova, T.A., and T.L. Madden. 1999. Blast 2 sequences: a new tool for comparing protein and nucleotide sequences. *FEMS (Fed. Eur. Microbiol. Soc.) Microbiol. Lett.* 174:247–250.
Thompson, J.D., T.J. Gibson, F. Plewniak, F. Jeanmougin, and D.G. Higgins. 1997. The ClustalX windows interface: flexible strategies for multiple sequence alignment aided by quality analysis tools. *Nucleic Acids Res.* 24: 4876–4882.
Turner, F.R., and A.P. Mahowald, 1977. Scanning electron microscopy of *Drosophila melanogaster* embryogenesis. II Gastrulation and segmentation. *Dev. Biol.* 57:403–416.
Young, P.E., T.C. Pesacreta, and D.P. Kiehart. 1991. Dynamic changes in the distribution of cytoplasmic myosin during *Drosophila* embryogenesis. *Development*. 111:1–14.
Zhang, J., C. Kong, H. Xie, P.S. McPherson, S. Grinstein, and W.S. Trimble. 1999. Phosphatidylinositol polyphosphate binding to the mammalian septin H5 is modulated by GTP. *Curr. Biol.* 9:1458–1467.